

Supporting information

Non linear magnetic behaviour around zero field of an assembly of superparamagnetic nanoparticles

Caroline de Montferrand^{1, 4}, Yoann Lalatonne^{1, 2}, Dominique Bonnin³, Laurence Motte^{1*},
Philippe Monod³

- 1- CSPBAT laboratory, UMR 7244 CNRS, University of Paris 13, France,
- 2- Service Médecine Nucléaire, Hôpital Avicenne, Bobigny, France
- 3- LPEM, UPR 5 CNRS, ESPCI ParisTech, France
- 4- Magnisense France, Paris, France

*Corresponding author

E-mail: laurence.motte@univ-paris13.fr, laurence.motte-torcheux@univ-paris13.fr

Telephone: ++33(0)148387707; Fax: ++33(0)148388528

Multiparametric Testing

In an attempt for multiparametric feasibility, two SPM probes : lab-made $\gamma\text{-Fe}_2\text{O}_3$ nanoparticles and commercial Estapor beads (1020/50, Merck), are mixed at different ratios. The iron concentration of the two ferrofluids was adjusted in order to obtain MIAplex® signatures at iso-intensity. Fig. S1A shows the MIAplex® signatures of the two kinds of particles.

Fig. S1B-D shows the experimental MIAplex® signatures measured by mixing the two kinds of particles in various proportions and the corresponding calculated curves. A rather good agreement is obtained between experimental and calculated curves. This confirms the high sensitivity of measuring $d^2B(H)/dH^2$ for characterization and separation purpose.

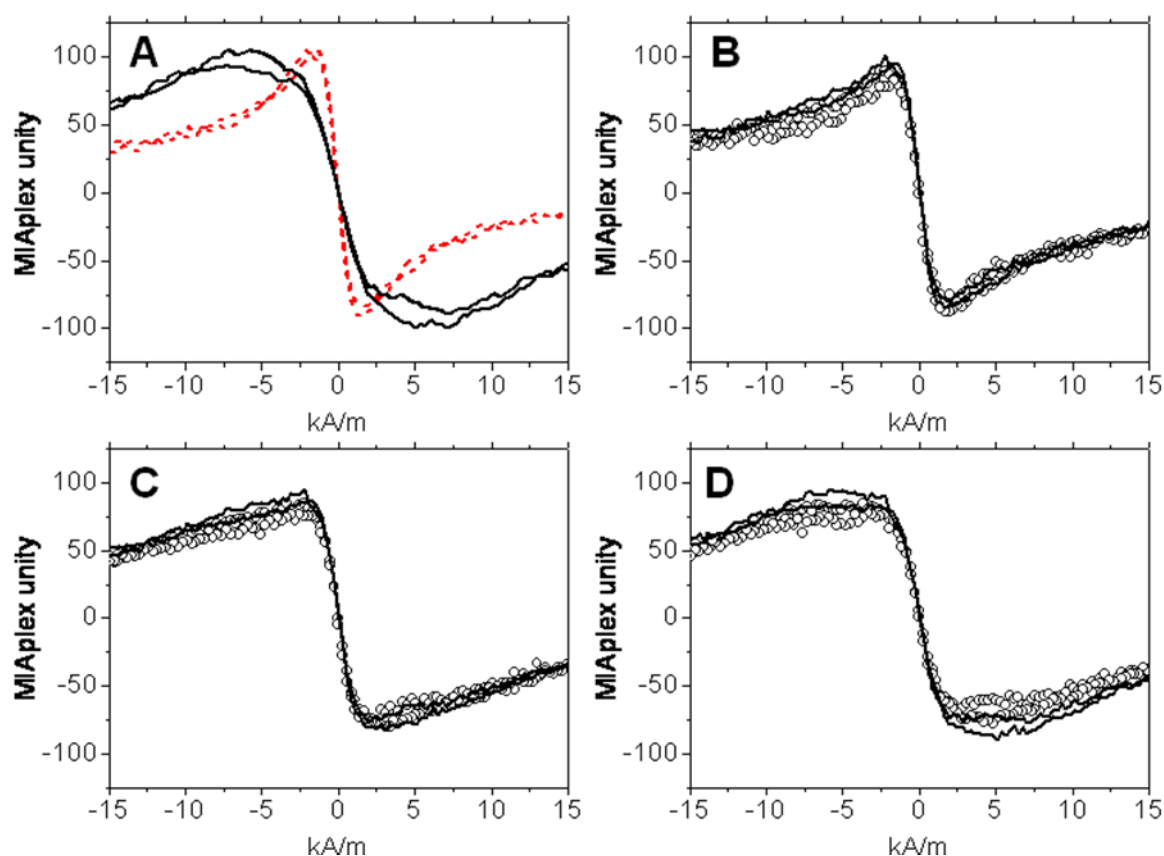


Figure S1: A : MIAplex® signature for nanoparticles (dashed line) and Estapor beads (solid line). **Experimental (open circles) and calculated (solid line) curves for 75%-25% (B), 50%-50% (C), and 25%-75% (D) nanoparticles-Estapor mixtures.**

Synthesis and characterization of $\gamma\text{Fe}_2\text{O}_3$ nanoparticles

Sodium n-dodecyl sulfate (99%, Alfa Aesar), dimethylamine solution (40%, Fluka), Iron (II) Chloride Tetrahydrate (Sigma Aldrich) were used as received. Water is purified with a Millipore system (resistivity 18.2 M Ω .cm).

Concerning lab-made nanoparticles, they are synthesized according to a procedure already described. Briefly, non coated $\gamma\text{Fe}_2\text{O}_3$ particles were synthesized by reaction of ferrous dodecyl sulfate with dimethylamine in water for two hours at 28°C¹. The nanocrystal surface is then functionalized with 5-

hydroxy-5,5-bis(phosphono)pentanoic acid, which allows a good dispersion in water of the nanoparticles. The nanoparticles surface is characterized via infrared spectroscopy (Fig. S1).

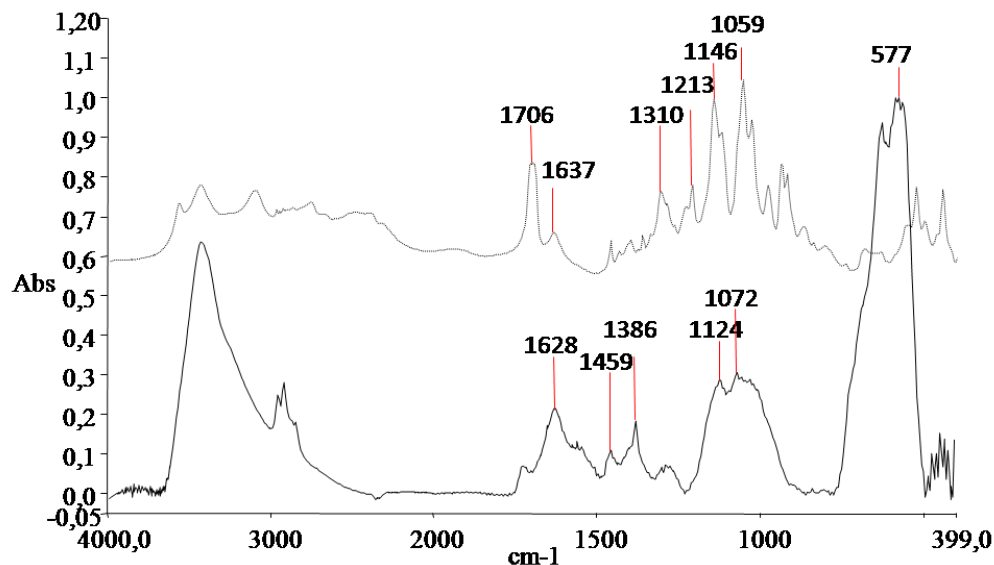


Figure S2: Infrared spectra of free 5-hydroxy-5,5-bis(phosphono)pentanoic acid (HMBP) (dotted line) and 10nm γ -Fe₂O₃@HMBP nanoparticles (solid line).

The spectrum of free HMBP molecule contains peaks at 1706cm⁻¹ (C=O), 1637cm⁻¹ (carboxylic C-O), 1309 and 1213cm⁻¹ (δ CH₂), 1146 and 1059cm⁻¹ (P-O). The spectrum of coated nanoparticles presents a very intense band at 577cm⁻¹ attributed to Fe and a large intense vibration band between 1150 and 950cm⁻¹ which corresponds to the P-O absorption band. Compared to free molecule, this modified band indicates that the molecule is bonded at the surface of the particle via the hydroxymethylene-bisphosphonate terminal function. The coating rate has been quantified via the P-O area band¹ and is evaluated as about 1500 HMBP molecules per nanoparticle.

Nanoparticles crystal size and structure were characterized by X-ray diffraction (XRD) and Transmission Electron Microscope (TEM). XRD pattern (Fig. S2 and S3) was measured with an X-ray powder diffractometer model X'Pert PRO, MPD, PANalytical, Almelo, the Netherlands, CoK α beam in Bragg Brentano geometry (y/y) was used combined with a fast detector based on real time multiple strip technology (X'Celerator). Crystal XRD size was determined with the Scherrer formula. TEM images were obtained using a FEI CM10 Microscope and samples were prepared by depositing a drop of nanoparticles suspension on carbon coated copper grids placed on a filter paper.

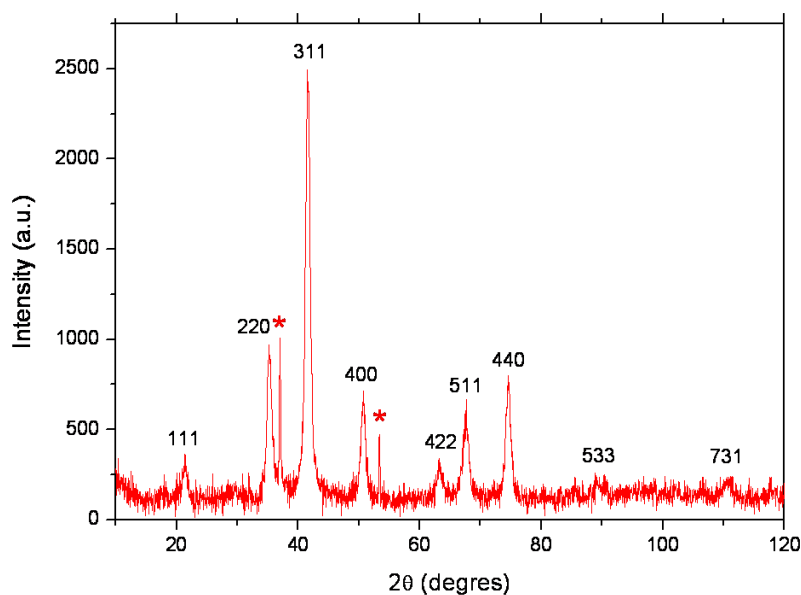


Figure S3: XRD pattern 10nm $\gamma\text{Fe}_2\text{O}_3$ @HMBP nanoparticles.

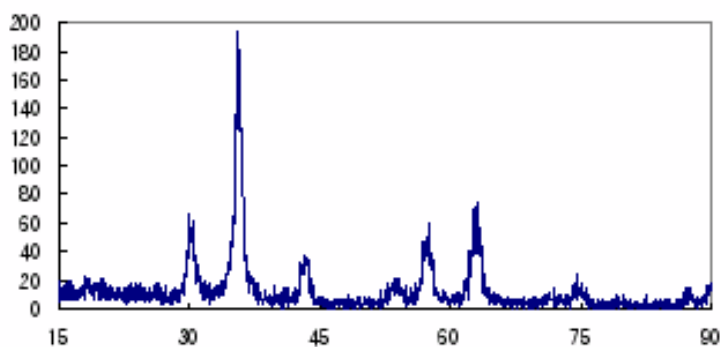


Figure S4: XRD pattern of Ferrotec Nanoparticles

The stars Figure S3 indicate the presence of NaCl residue. Phases identified are maghemite $\gamma\text{Fe}_2\text{O}_3$ and magnetite Fe_3O_4 (EVA software (version 13, Bruker-AXS, Karlsruhe, Germany, 1996–2007) and JCPDS-International Centre for Diffraction Data Powder Diffraction File (PDF-2, JCPDS-ICDD, Newtown Square, PA)). Crystal size is determined via the Scherrer equation and is 9.9nm.

The median diameter d_0 and standard deviation w are deduced from TEM data measurements, simulating the diameter d distribution with a lognormal function $g(d)$ described in equation (1).

$$g(d) = \frac{1}{\sigma d \sqrt{2\pi}} \exp\left(-\frac{\left(\ln \frac{d}{d_0}\right)^2}{2\sigma^2}\right) \quad (1)$$

The parameter σ is related to the standard deviation w by the relation (2).

$$\sigma = \sqrt{\ln\left(1 + \left(\sqrt{1 + 4\left(\frac{w}{d_{med}}\right)^2} - \frac{1}{2}\right)\right)} \approx \sqrt{\ln\left(1 + \left(\frac{w}{d_{med}}\right)^2\right)} \quad (2)$$

Magnetic properties of $\gamma\text{Fe}_2\text{O}_3$ nanoparticles

Magnetic properties were measured using a superconducting quantum interference device (Quantum Design SQUID Magnetometer MPMS-5T) at 300 K and the MIAplex® technology. Samples measured with SQUID are liquid suspensions in water, 0.5wt%, conditioned in silicone capsules supplied by Plastem S.A. Concerning the MIAplex®, samples are also liquid suspensions in water 0.5wt% and 2wt%, conditioned in 500 μL Eppendorf.

The saturation magnetization is obtained by the extrapolation of the plot of magnetization vs the inverse of the field at the origin² (Fig. S4).

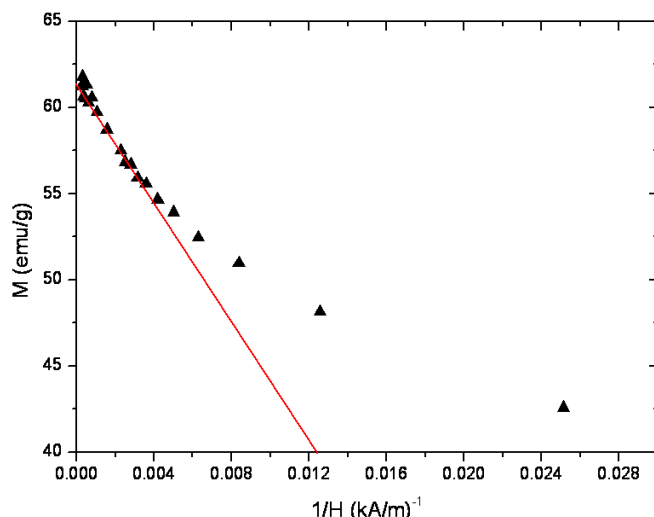


Figure S5: Magnetization M as function of $1/H$.

The red line is the asymptote when $1/H$ tends to zero. The intersection between this asymptote and y-axis is the experimental saturation magnetization M_{sat} .

Considering a core-shell system, the spin canting thickness e and the corresponding magnetic size ($d_0 - 2e$) are deduced from the equation (2)³.

$$M_{\text{sat}} = M_{\text{satbulk}} \times \left(\frac{d_0 - 2e}{d_0} \right)^3 \quad (2)$$

For the lab-made nanoparticles with $d_0 = 10.5\text{nm}$ as TEM diameter and $M_{\text{sat}} = 61\text{emu/g}$, we calculate a magnetic size of $d_m = 9.6\text{nm}$, corresponding to a non magnetic layer of $e \approx 0.45\text{nm}$. We estimate the contribution of the shell in the total volume of the particles from the equation (3).

$$\%(V_{\text{shell}}) = 100 \times \frac{V_{\text{shell}}}{V_{\text{crystalline}}} = 100 \times \frac{V_{\text{crystalline}} - V_{\text{magnetic}}}{V_{\text{crystalline}}} = 100 \times \frac{d_0^3 - d_m^3}{d_0^3} \quad (3)$$

We so obtained a shell contribution of 24% of the particle volume.

The Langevin model of superparamagnetism⁴ can be used to describe the non-linear magnetization curve of the nanoparticles, assuming that particles do not interact, by the equation (4).

$$\frac{M}{M_{\text{sat}}} = \coth\left(\frac{v\rho M_{\text{sat}}\mu_0 H}{k_b T}\right) - \frac{k_b T}{v\rho M_{\text{sat}}\mu_0 H} \quad (4)$$

v is the volume of the magnetic core, ρ is the particle density ($4900\text{kg}\cdot\text{m}^{-3}$ for maghemite), M_{sat} ($\text{emu}\cdot\text{g}^{-1}$) is the saturation magnetization of the particle, T is the sample temperature in Kelvin (taken to be 300 K), μ_0 is the permeability of vacuum ($4\pi \times 10^{-7} \text{H}\cdot\text{m}^{-1}$), H is the applied field (in $\text{A}\cdot\text{m}^{-1}$) and k_B is the Boltzmann constant, $1.38 \times 10^{-23} \text{J}\cdot\text{K}^{-1}$. As to model the experimental magnetic data, we have used the Langevin equation weighted by a lognormal function (equation 1).

The experimental curves at high and medium magnetic field ranges are fitted with 1 Langevin equation weighted by log-normal distribution.

At low magnetic field range, the experimental curve are fitted with the sum of 2 Langevin equations weighted by log-normal distribution and corresponding to separate contributions.

The second derivative of the magnetization fit at high and medium magnetic field ranges is compared with the MIAplex® signature (Figure S5).

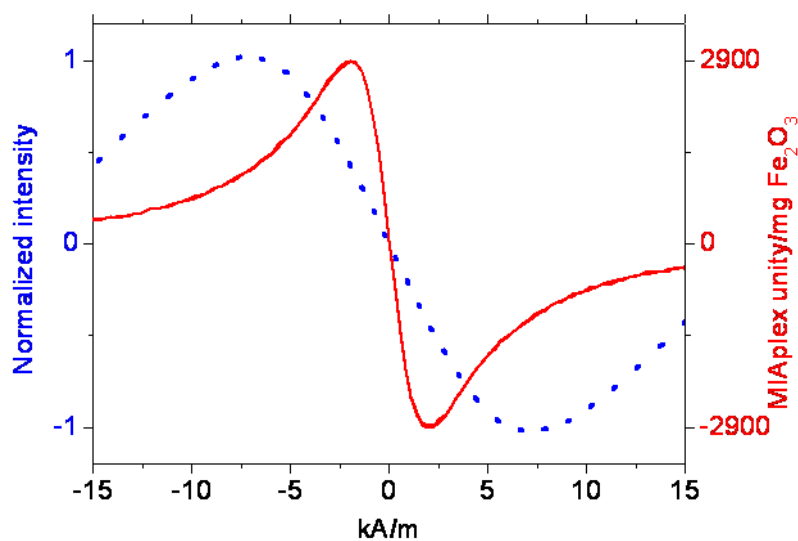


Figure S6: Second derivative of the magnetization fit at high and medium magnetic field range (dotted line) superposed with the MIAplex® signal (solid line).

The second derivative of the high and medium magnetic field magnetization fit presents a peak-to-peak line width in field $\Delta H_{\text{pp}} = 14.4 \pm 0.2 \text{ kA}\cdot\text{m}^{-1}$ which is about 3.7 times bigger than the MIAplex® signature ($\Delta H_{\text{pp}} = 3.9 \pm 0.1 \text{ kA}\cdot\text{m}^{-1}$).

1. Lalatonne, Y. et al. Bis-phosphonates-ultra small superparamagnetic iron oxide nanoparticles: a platform towards diagnosis and therapy. *Chemical Communications*, 2553-2555 (2008).
2. Caizer, C. Saturation magnetization of $[\gamma]\text{-Fe}_2\text{O}_3$ nanoparticles dispersed in a silica matrix. *Physica B: Condensed Matter* **327**, 27-33 (2003).
3. Millan, A. et al. Surface effects in maghemite nanoparticles. *Journal of Magnetism and Magnetic Materials* **312**, L5-L9 (2007).
4. du Trémolet de Lacheisserie, E. *Magnétisme Fondements Vol. I.* (Grenoble Science, Grenoble; 2000).